FACULDADE DE ENGENHARIA DA UNIVERSIDADE DO PORTO

Development of an ns-3 based Simulation Tool for TCP/IP Maritime Wireless Networks

Tiago Telmo Pinto de Oliveira

Mestrado Integrado em Engenharia Eletrotécnica e de Computadores

Supervisor: Manuel Ricardo (PhD)

Co-Supervisor: Rui Campos (PhD)

July, 2015

U.PORTO
FEUP FACULDADE DE ENGENHARIA UNIVERSIDADE DO PORTO

MIEEC - MESTRADO INTEGRADO EM ENGENHARIA ELETROTÉCNICA E DE COMPUTADORES | **2014/2015**

A Dissertação intitulada

"Development of an ns-3 Based Simulation Tool for TCP/IP Maritime Wireless Networks"

foi aprovada em provas realizadas em 21-07-2015

o júri

Presidente Professor Doutor Paulo José Lopes Machado Portugal
Professor Associado do Departamento de Engenharia Eletrotécnica e de Computadores da Faculdade de Engenharia da Universidade do Porto

Professor Doutor Jorge Botelho da Costa Mamede
Professor Adjunto do Departamento de Engenharia Electrotécnica do Instituto Superior de Engenharia do Porto

Professor Doutor Manuel Alberto Pereira Ricardo
Professor Associado do Departamento de Engenharia Eletrotécnica e de Computadores da Faculdade de Engenharia da Universidade do Porto

O autor declara que a presente dissertação (ou relatório de projeto) é da sua exclusiva autoria e foi escrita sem qualquer apoio externo não explicitamente autorizado. Os resultados, ideias, parágrafos, ou outros extratos tomados de ou inspirados em trabalhos de outros autores, e demais referências bibliográficas usadas, são corretamente citados.

Tiago Oliveira

Autor - Tiago Telmo Pinto de Oliveira

Faculdade de Engenharia da Universidade do Porto

Abstract

Wireless communications are expanding beyond land and recent research works have been trying to bring wireless communications to other environments such as the maritime environment.

For a long time the communications in the ocean have been made using analog channels, which have narrow bandwidth and offer a very limited set of features. Communications via satellite are an alternative but too expensive for most of the ships. Attempting to develop a cheaper and more feasible solution has its challenges, as there is no open source and accurate way to simulate possible solutions, thus making it necessary to spend money and time with the planning of sea trials.

The goal of this MSc thesis was to develop an open source simulation tool, enabling the simulation of TCP/IP maritime wireless networks, including the simulation of the signal propagation in the maritime environment and the ocean surface movement. The simulation results were compared with experimental results found in literature and obtained in previous MSc thesis developed at INESC TEC, allowing to validate the new simulation tool.

Acknowledgments

First, I would like to thank my supervisor Prof. Manuel Ricardo for giving me the opportunity of developing this research work at INESC TEC. A special thanks to Dr. Rui Campos for all the support and suggestions given, which were essential in the development of my thesis. Also, thanks to Sérgio Conceição, my non-official supervisor, for all the help with the ns-3 and thesis in general.

Thanks to my friends for all the support and great moments experienced through, not only this work, but also the entire course.

Finally, I would like to thank my family for all the support and motivation given along the years, specially my parents and brother, who were always there for me.

Tiago Oliveira

"Either write something worth reading
or do something worth writing."

Benjamin Franklin

Contents

List of Figures

List of Tables

Listings

Acronyms

BER	Bit Error Rate
FER	Frame Error Rate
IEEE	Institute of Electrical and Electronics Engineers
IP	Internet Protocol
HF	High Frequency
LOS	Line of Sight
MARBED	MARitime wireless networks testBED
MF	Medium Frequency
MRPT	MAC-based Routing Protocol for TRITON
MSc	Master of Science
NANET	Nautical Ad-hoc Network
ns-3	Network Simulator 3
OFDM	Orthogonal Frequency-Fivision Multiplexing
OLSR	Optimized Link State Routing Protocol
QoS	Quality of Service
RSSI	Received Signal Strength Indication
TCP	Transmission Control Protocol
TRITON	Trimedia Telemetric Oceanographic Networks
UDP	User Datagram Protocol
VHF	Very High Frequency
VoIP	Voice over IP
WiMAX	Worldwide Interoperability for Microwave Access
WISEPORT	WIreless-broadband-access for SEaPORT

Chapter 1

Introduction

1.1 Context

In a maritime environment, the wireless communications in narrowband are the most dominant. To support voice communications between ships and between ships and land, HF/VHF analog channels are typically used. Only near shore it is possible to use cellular networks (3G/4G) as an alternative. So the communications are limited to near shore or to the utilization of communications systems via satellite, which have monthly costs that most of the ships cannot afford [9].

On the other hand, the utilization of autonomous surface vehicles in maritime environment has been researched in scenarios of environmental monitoring and search and rescue, in which wireless communications are a central part to guarantee the cooperation between vehicles, cooperation with human operators, and communications with land stations.

The need for a better and less expensive way to have wireless communications in the maritime environment is needed. Projects, such as TRITON [10] and NANET [6], have been developed in order to improve wireless communications in the sea environment, thus making it more affordable. However, the maritime environment presents different characteristics when compared to the terrestrial environment, thus requiring the design and test of new communications solutions.

1.2 Motivation

In recent years, several projects have emerged in the wireless maritime communications area, in order to improve some maritime activities, such as fishing, by giving ships the capability of communicating with each other and with land in an affordable way. However, the signal propagation characteristics in the sea vary depending on the sea movement, which affects the signal propagation in different ways, making it hard to test a possible solution with constantly changing scenarios. In addition, the implementation of testbeds in the sea has some logistic issues, such as the cost associated to the implementation and maintenance of the testbed and the authorizations to perform those tests.

An alternative method to test out the different scenarios and overcome those limitations is by using a simulator, which allows to define the characteristics of the signal propagation and easily controlling the scenarios, like defining the state of the sea. Also, with a simulator, we can easily repeat a test for a specific scenario, something that it is not possible with a real test, as we cannot run the test twice in the same exact conditions. Finally, the use of a simulator will allow to evaluate whether a possible solution is viable and if it is worth to do a real test.

There are already some network simulators available, but they do not enable the simulation of maritime wireless networks or are closed source. An open source simulation tool is thus lacking.

1.3 Objectives

The main goal of this work is to develop a simulation tool for TCP/IP maritime wireless networks, based on ns-3, which lacks maritime simulation models. The simulation tool will focus on propagation and mobility layers in the ns-3 architecture. Concerning the propagation layer, the developed tool should allow to simulate maritime wireless communications, and therefore a propagation model using the appropriate pathloss model should be developed. As for the mobility layer, the simulation tool needs to recreate the scenario of the maritime communications, where the nodes are oscillating according to the sea wave movement. In order to achieve that, the mobility model must implement wave movement models that will vary the nodes height along the simulation. At the end of this work, this tool shall be tested with the comparison of the results obtained using the new simulation tool with the experimental results obtained in previous works.

1.4 Contributions

The main contribution of this dissertation is a new simulation tool for TCP/IP maritime wireless networks based on ns-3. With this tool, existing and future maritime networking research can be tested before going to the field, allowing researchers to conclude whether their solutions are feasible before deploying them in the real maritime environment. The new developed simulation models enhance ns-3 with the capabilities of performing maritime simulations.

1.5 Structure

This document is organized in five chapters. Chapter 2 presents the state of the art. Chapter 3 describes the developed simulation tool for maritime wireless networks. The validation of the developed simulation tool is reported in Chapter 4, including the description of the simulation setups and the analysis of the simulation results in comparison with experimental results obtained in sea trials. Finally, we draw the major conclusions and discuss possible future work in Chapter 5.

Chapter 2

State Of The Art

In this chapter, we present the state of the art on maritime wireless networks. We start by defining some concepts about the maritime communications environment. Next, we present the two-ray maritime propagation models and the models of the sea surface movement. After that, some communications solutions for maritime environment are presented, with one of them having a proprietary simulation framework, that is object of analysis in the last section, where we present some network simulators, including ns-3 that will be the basis of the development of the simulation tool for maritime networks. Finally, we present the MARBED testbed and some experimental results that will be used for validating the new simulation tool.

2.1 Maritime Communications Characterization

When comparing the maritime environment with the land environment, there are some additional challenges regarding the wireless communications. In [11] the authors state that the maritime communication environment is mainly characterized by the sea surface movement, the radio propagation and the Fresnel effect.

The constant sea wave movement leads to an unstable link quality, since the sea waves causes ships (and thus the antennas placed on them) to move in various ways, continuously changing the antenna orientation and height. Since the distance between ships is long in comparison with the antenna heights, the antenna gains will suffer small variations with the continuous change of the ship height (and subsequently the antenna height). However, the changes in the orientation of the antenna are more significant because the signal strength is more affected by the antenna tilt [1]. Figure 2.1 demonstrates these effects, as in a), with the height variations, the signal propagation direction is barely affected, as in b) the tilt substantially changes the signal propagation of the antennas.

The radio channel properties are closely related to the propagation environment. In a maritime environment the signal propagation is affected by the propagation over water, surface multi-path reflection, and blockage of the signal by an obstacle like near ships, rocks and cliffs or just by wave occlusion. So, depending on the conditions, the radio propagation will be more or less affected.

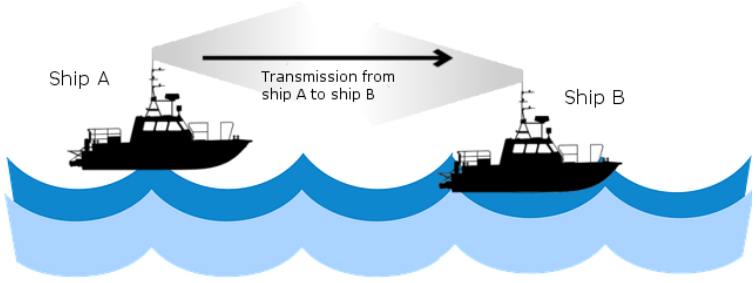

a) Variations in path-loss in the null region due to the height variation of the antennas.

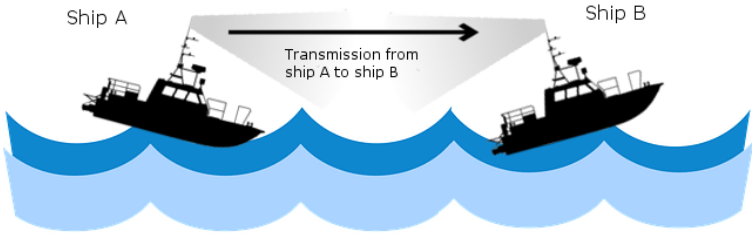

b) Variations of the gains due to the tilt of the antennas.

Figure 2.1: Variations in received signal strength due to the sea waves (adapted from [1])

The Fresnel effect consists in a significant reduction of the received signal, when the signal bumps into an obstacle inside of the first Fresnel zone. This effect can be minimized by using an antenna with proper height or suitable frequency.

2.2 Two-Ray Propagation Model

As we saw in Section 2.1, the radio channel properties in a maritime environment is different when compared with a land environment, since the signal is affected by distortions of reflection and refraction by the surface of the sea and also because of the movement and tilt of the ship (plus the antenna equipped in it) due to the waves movement. So, it is important to have propagation models to describe the signal behaviour in this kind of environment.

In [2] the authors presented a two-ray pathloss model, based on the direct ray and the reflected ray, which they argue to be able to fit the actual behavior of the observed maritime channel. To evaluate the effects of this pathloss model, they did a simulation study carried out using the OPNET simulator, where they aimed at comparing the throughput at IP level obtained using different pathloss models implemented in OPNET. The simulation consisted in placing an antenna in a location at 30 meters above the sea surface, with a gain of 17 dBi, transmitting at 35 dBm of power and another antenna, omnidirectional and with gain 11 dBi, placed on a ship, at approximately 10 meters height. The system performance was evaluated in terms of throughput using UDP instead of TCP (to avoid congestion algorithm's limitations) and in terms of RSSI.

The RSSI was measured for different distances; the results are presented in Figure 2.2. Up to a 5 km distance, the RSSI has some periodical fading deep holes, and after the 5 km, the RSSI stabilized, having a linear decrease of less than 1 dB/km, until 19 km far from shore, where several synchronization problems were detected, making it impossible to communicate with the base station, on land.

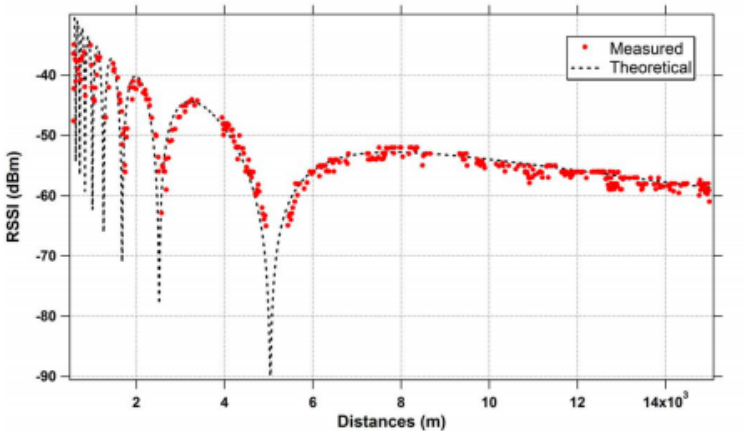

Figure 2.2: Theoretical and Measured RSSI for different distances [2]

Considering the experimented RSSI, a two-ray radio propagation model was proposed, that fits the measured data:

Signal Power Received:

$$P_r = \frac{P_t G_t G_r}{L_2 ray} \tag{2.1}$$

Proposed two-ray Pathloss Model:

$$L_2 ray = \frac{L_f s}{\beta} \tag{2.2}$$

Free Space Pathloss Model:

$$L_f s = \left(\frac{4\pi d}{\lambda}\right)^2 \tag{2.3}$$

Reflection Coefficient:

$$\Gamma(\theta_i, n_1, n_2) = \frac{n_1 \cos\theta_t - n_2 \cos\theta_i}{n_1 \cos\theta_t + n_2 \cos\theta_i} \tag{2.4}$$

Angle of Transmitted Wave :

$$\theta_t = \arcsin\left(\frac{n_1}{n_2} \sin\theta_i\right) \tag{2.5}$$

$$\beta = 1+\Gamma(\theta_i,n_1,n_2)^2-2\Gamma(\theta_i,n_1,n_2)\cos\left(\frac{4\pi h_t h_r}{\lambda d}\right) \quad (2.6)$$

In Equation 2.1, P_t, G_t and G_r represent the transmission power, the transmitter antenna gain and the receiver antenna gain respectively. L_2ray represents the proposed two-ray pathloss model and is given by Equation 2.2, where L_fs represents the free space pathloss model evaluated according to Equation 2.3 and β is given by Equation 2.6. $\Gamma(\theta_i,n_1,n_2)$ is the reflection coefficient for a parallel polarized electromagnetic wave, represented by Equation 2.4, where n_1 is the refraction index of air ($\cong 1$) and n_2 is the refraction index of water ($\cong 1.333$), θ_i is the wave angle of incidence and θ_t is the angle of transmitted wave, given by Equation 2.5. The height of the transmitter and receiver antenna are represented by h_t and h_r, respectively, and d is the distance between the base station and the ship and λ represents the wavelength of the radio wave.

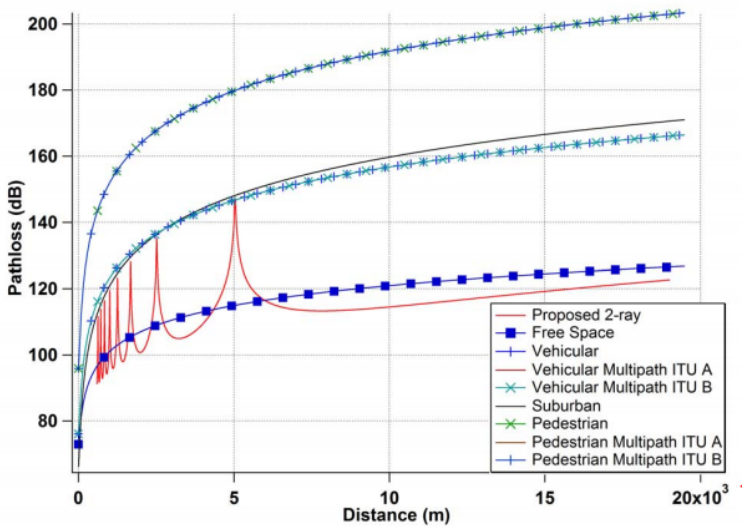

Figure 2.3: Simulated Pathloss Models Results [2]

Figure 2.3 shows the comparison between the proposed two-ray pathloss model and the other models available in the OPNET simulator. None of the other models captured the pathloss peaks that were observed in the measured data and also captured by the proposed two-ray model, due to the specific sea characteristics that those models do not predict. The free space model is the one that gets closer to the developed two-ray model, except in the part of the pathloss peaks.

In [1] the authors present another two-ray model for maritime communications. This model is represented by Equation 2.7, and only takes into account the distance, d, between transmitter and receiver, the effective heights of transmitter, h_t, and receiver, h_r, and the wavelength of the radio transmission, λ.

$$L(h_t,h_r,t) = 10\log\left(\frac{\lambda^2}{(4\pi d)^2}\left(2\sin(\frac{2\pi}{\lambda}\frac{h_t h_r}{d})\right)^2\right) \tag{2.7}$$

As the distance between the antennas increases, the angle in the sine term decreases, and so, there is less fluctuation in the path loss value, meaning that the antenna's gain are responsible for the quality of the link at such distances. On the other hand, for smaller distances, the path loss fluctuates according to the antenna's height variations, which can result in path loss peaks in comparison with the free-space pathloss model, as shows Figure 2.4.

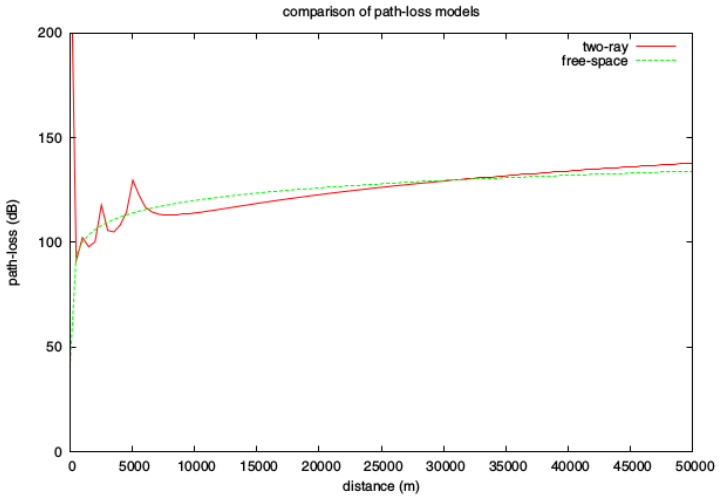

Figure 2.4: Two-ray pathloss model versus free-space pathloss. [1]

2.3 Maritime Oscillation Models

As we saw in Section 2.1, the sea wave movements causes ships and their equipped antennas to be constantly moving and tilting, thus affecting the quality of the link. In order to simulate the maritime environment it is necessary to have models that represent the sea wave motion.

The simplest way to model a sea wave is through a sine wave. The travelling sine wave [12], fits best in the representation of the sea wave propagation, as it represents the sine wave travelling in two spatial directions. Equation 2.8 represents the travelling sine wave, where the height, y, depends on both X coordinate and time.

$$y = A\sin(kx - \omega t) \tag{2.8}$$

Where k represents the number of wavelengths per unit length, or wave number, which can be translated into $k = 2\pi/\lambda$. The angular frequency, ω, is given by $2\pi f$, where f stands for the wave

frequency, which is equal to $1/T$, with T being the wave period.

The sine wave model is good for representing the sea wave when the sea is in a calm state. However, for less calm states, the waves have larger amplitudes, thus making it less viable to represent them via the sine wave.

A better way to represent such sea states is by means of the trochoid wave form, which can be defined as the curve traced out by a point on a circle as the circle rolls along a line. This wave form is more realistic than the simple sine waveform [4], as it becomes a sharpened crested shape in this situation. In the case of calm sea, the trochoid presents a smooth profile, that approaches the sine wave shape, but it is possible to see that this shape is different, with a narrowing of the peaks of the trochoid compared to the sinusoid. This narrowing or steepening of the peak becomes more pronounced as the wave amplitude increases, as shown in Figure 2.5.

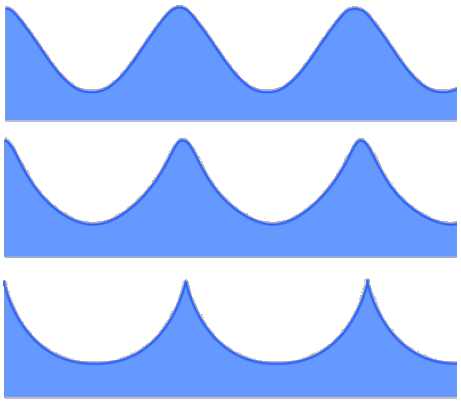

Figure 2.5: Trochoidal Wave Shape as the amplitude increases for a given wavelength [3]

Equations 2.9 and 2.10 represent the parametric equations of the trochoid wave, in which the trajectory of a water particle is expressed as a circle of radius r around its reference location at rest, $(x0, z0)$ [13]. The actual location, at time t, is represented by (x, z), the pulsation with the sea wave frequency f is given by $\omega = 2\pi f$ and $k = 2\pi/\lambda$ the wave number with respect to the sea wave length of λ.

$$x = x_0 + r\sin(\omega t - kx_0) \tag{2.9}$$

$$z = z_0 + r\cos(\omega t - kz_0) \tag{2.10}$$

Equation 2.11 represents an approximation of the travelling wave to the trochoid wave model, where λ, T, and H are the average wave length, the average wave period, and the significant wave height.

$$y = \frac{\lambda}{2\pi} - \frac{H}{2} \times \cos\left(\frac{x}{\lambda} - \frac{t}{T}\right) \tag{2.11}$$

The trochoid equation is just a two-dimensional representation of the sea wave, as the x-axis coincides with the direction of the wave propagation. Yet, the sea surface movement cannot be

represented by a single wave, but rather several waves, moving simultaneously. The surface of the sea is actually made up by a finite sum of simple waves [13]. The height z of the water surface on the grid point (x,y) at time t is expressed by Equation 2.12.

$$z(x,y,t) = \sum_{i}^{n} A_i trochoid(k_i(xcos\theta_i + ysin\theta_i) - \omega_i t + \varphi_i) \quad (2.12)$$

Where n is the number of wave trains, A_i the amplitude, k_i the wave number, θ_i the direction of wave propagation on the xy-plane and φ_i is the phase. As shown in Figure 2.6, the greater the product kr is, the more sharpened waves will be.

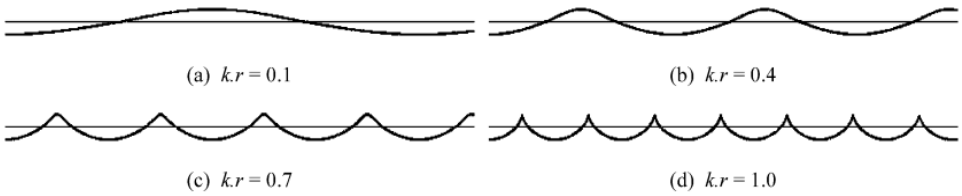

Figure 2.6: Shape of a trochoid according to the product kr [4]

Both sine and trochoid wave models, depend on the sea wave characteristics, such as its length, period and amplitude. The Pierson-Moskowitz sea states [1] classify the sea in 10 levels, as shown in Table 2.1. Using this table, the user can specify the sea condition simply by indicating a sea state level.

Sea State Level	Significant height (m)	Avg. Period (sec)	Avg. Wave Length (m)
0	0.09	0.5-1	0.46-0.61
1	0.15-0.3	1.5-2.0	3-5
2	0.46-0.91	2.5-3.5	6-12
3	1.07-1.52	3.5-4.5	14-20
4	1.83-2.29	5.0-5.5	24-30
5	2.44-3.66	5.5-7.0	32-48
6	4.27-6.10	7.5-9.0	56-80
7	7.62-12.19	10.0-12.5	100-160
8	13.72-18.29	13.0-15.0	180-237
9	21.34-27.43	16.5-18.5	280-360

Table 2.1: The Pierson-Moskowitz Sea State Table

As we can see for the first levels, we can say that the sea is in a calm state, with the waves less than 2 meters high. Above level 6, the sea becomes more severe, being able to reach 30 meters high, in case of level 9.

2.4 WiMAX on Maritime Communications

The WiMAX protocol is an IEEE 802.16 standard that provides wireless broadband access of up to 50 km, 2 to 66 GHz range, network discovery and selection, QoS management, security and the fast user mobility (although in the maritime situation, the ships will not move as fast as a land vehicle, so there will be a better communication). Regarding this protocol, there are some experimental studies and in this section we will be presenting two of them.

In [5] are presented path loss measurements for different antennas height, using WiMAX 5.8 GHz, in a sea port. For transmission it was used a omnidirectional antenna with 12 dBi gain transmitting at 0 dBm, with the output signal further amplified using a 30 dB amplifier. It was performed measurements considering the transmission antenna placed at different heights (4 m, 76 m and 185 m). The same omnidirectional antenna was used as the receiver, placed on a boat and mounted 8 meters from sea level.

In the first case, where the transmission antenna's height was 185 m, the antenna was placed in a tall building, near the shore (approximately 1 km). Figure 2.7 shows the results from the measurements in this case for distances between 2 and 2.5 the received power varied less when compared to distances > 2.5, which resulted from the fact that between 2 and 2.5 the receiver had a good LOS to the transmitter.

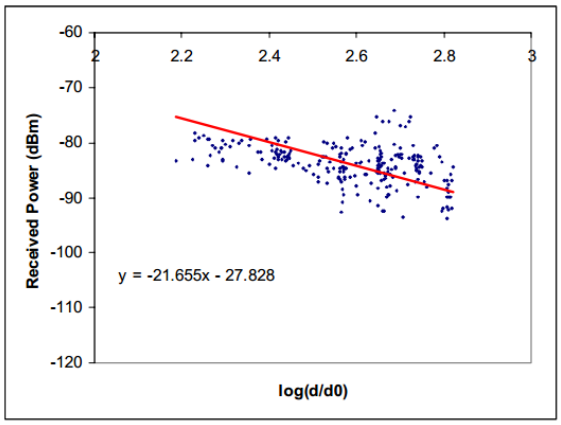

Figure 2.7: Received Power for Antenna with 185 m heigh [5]

The second case, where the the transmission antenna's height was 76 m, the antenna was placed in a light house, half kilometer away from the shore. Figure 2.8 shows the results, which are close to the two-ray pathloss model.

In the last case, where the the transmission antenna's height was 4 m, the antenna was placed on a tripod which was about 3 m from the ground level. Unlike previous cases, the LOS was not dominant during the measurement. Figure 2.9 displays the results for this case, where, when $d < d_A$ the path loss exponents are close to that of free space, but when $d > d_A$ the path loss exponents are much larger than that predicted by the two ray model, meaning that the signal will attenuate very rapidly at distance $d > d_A$ and this will limit the coverage zone of WiMAX.

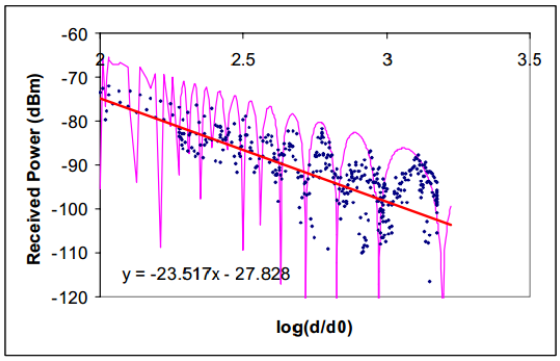

Figure 2.8: Received Power for Antenna with 76 m heigh [5]

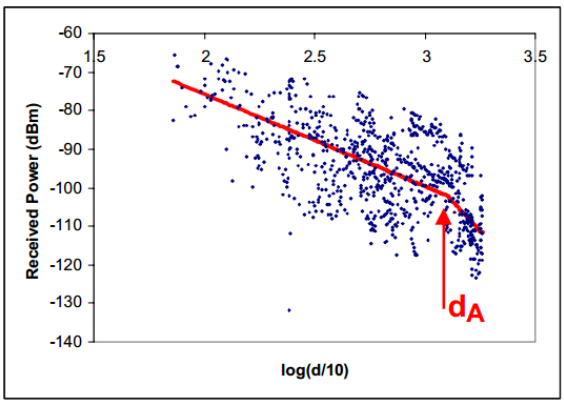

Figure 2.9: Received Power for Antenna with 4 m heigh [5]

In [14] is presented the performance of fixed WiMAX at 5.8 GHz, in a sea port environment in the presence of multipath, Doppler shift, and boat's rocking. Measurements of multipath and Doppler shift were carried out in order to understand BER results from a fixed WiMAX equipment, thus allowing an analysis of the impact of these effects in the communication link.

The measurements were carried out between 1 and 2 km from the shore. The sea condition was quite calm and there were no large waves. A fixed WiMAX equipment was set as a host and placed on the shore, and the other one was set as a client on a diving boat. At host site, it was used a 16 dBi sector antenna with 60^{o} horizontal beam width placed on a tripod, which was 3 m high from the ground. At the client site, it was used two different antennas, placed on top of a pole which was 5.5 m from sea surface. The first one, was an omnidirectional antenna with 12 dBi, as for the second it was equal to the antenna used in the host.

The measurements when using the omnidirectional antenna at the client site, allowed to check the presence of an irreducible BER floor caused by the multipath and/or the Doppler shift. In order to investigate what caused the irreducible BER floor, were carried out multipath and Doppler shift measurements, that allowed to conclude that Doppler shifts caused irreducible BER and FER floor in the fixed WiMAX mounted on a moving vessel in the sea port. The measurements showed that

it is possible to mitigate this problem with a sector antenna. The boat's rocking was also a factor that could increase BER, especially when the link was marginal.

2.4.1 WISEPORT

Launched in Singapore in March 2008, the WISEPORT project [15] was the world's first mobile WiMAX ready seaport. WISEPORT aims to provide high bandwidth, low-cost and secure communications channels for ships within 15 km from Singapore's southern coastline. Involved in this project were the Maritime and Port Authority of Singapore, Infocomm Development Authority and QMax Communications Pte Ltd, with this last one being the responsible for the mobile WiMAX services, offering download access speed ranging from 512 kbps to 8 Mbps. Under the project, at least six WiMAX base stations were set up, each having estimated coverage range of up to 15 km extending into the port waters, allowing to cover the southern port waters, and also to cover the container terminals, oil terminals and shipyards at four maritime hotspots in south Singapore.

This allowed activities like regulatory filings, broadband communications, live remote video and security surveillance, real-time access to navigational data and Internet-based applications, such as access personal emails, make VoIP calls, and video conferencing, that could only be done onshore, to be replicated offshore.

2.4.2 TRITON

The TRITON project [10] aimed to develop a maritime mesh communication infrastructure that is able to provide high bandwidth and acceptable QoS levels to enable a multitude of new high speed applications, using the IEEE 802.16 mesh and IEEE 802.16e standards.

In this project, three routing protocols were studied, but none of them were ideal for maritime wireless mesh networks, so they proposed a new routing protocol, specialized in maritime communications. This protocol, named MRPT, is a proactive routing protocol that uses WiMAX mesh MAC control messages to propagate routing information from the land station to the ships. This proactiveness is achieved without much control overhead compared to OLSR because additional routing messages are piggybacked on existing MAC control messages, allowing multiple routes to be readily available in a tree structure, such as a newly arrived node can join the network immediately, reducing the initial packet delay. Also, there are alternative routes for route switching when an existing link is broken, thus increasing the network robustness.

2.5 WetNet

The WetNet architecture is based on the IEEE 802.11, and it consists on a high-data rate network-centric protocol with extended range capability, operating at various user-selectable frequencies including military and commercial bands. In [16], the authors state the benefits of the WetNet technology:

- **Open Systems, Network-based Architecture** - provides network-centric operation in the various frequency bands, compatible with standard addressing;
- **High capacity bi-directional half-duplex bandwidth** - with effective transports rates of 6 Mbps at approximately 350 m, with autonomous rate adjustments maxing the supportable data rate per link conditions;
- **Standard networking interfaces** - standard Ethernet-based interfaces;
- **Robust data/messaging capabilities** - CRC data protection and integrated encryption, with guaranteed ARQ delivery, and advanced OFDM waveform with convolutional coding and scrambling.

In that same work, WetNet was evaluated in different scenarios, with one of them being the boat-to-shore. Regarding this scenario, two nodes supporting a 802.11 transceiver, with a 10 Watt power amplifier for the transmit path, a low noise amplifier for the receive path, were used. A sector antenna with 19.6 dBi of gain, located at 48 m, on shore, and an omnidirectional antenna with 6 dBi of gain, on the boat, at 4.5 m above the sea level, were used to collect data. In this scenario, the field-testing of the WetNet showed 6 and 12 Mbps rates, available at 64 km.

2.6 NANET

NANET [6] is mesh/ad-hoc network solution for maritime communication. The goal of this solution is to have a low cost network, with enhanced transmission speed, using a similar topology as Vehicular Ad hoc Network, thus allowing peer-to-peer communications between ships, without needing base stations. Figure 2.10 represents the two architectures presented in that work, one for the shore (on the left), and the other one for the sea (on the right).

In the shore architecture if a ship is in the coverage area of a radio access station (RAS), it is able to communicate directly with it, but if the ship is outside the coverage of the RAS, then it is configured a mesh network with other ships and/or buoy access point, in order to reach the RAS.

In the sea architecture, there is no base station available in the network, because it is too far from the land, and it is not possible to create a link from a ship to RAS by multi hop, like in the first case. So, if there is no ship or buoy access point within the coverage to create a link, the solution is to use a modem in the MF/HF band, so it can connect directly to the base station in the land.

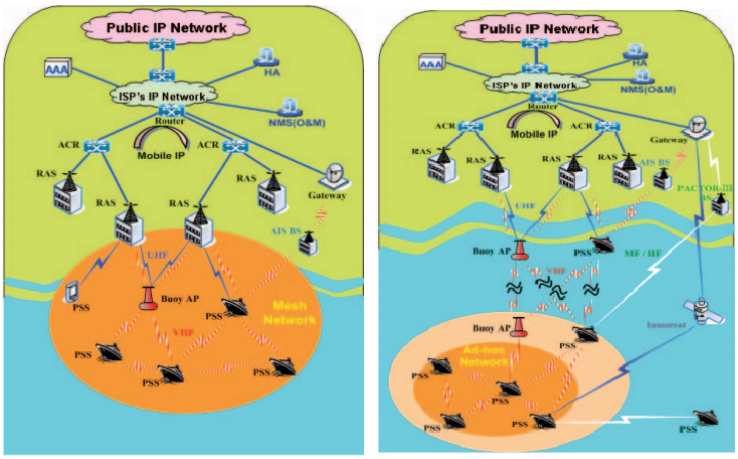

Figure 2.10: Shore and Sea Arquitectures [6]

2.7 MARBED

MARBED is a testbed developed at INESC TEC, aimed to support experimental research on maritime wireless networks. This testbed consists of two land stations and eight sea nodes deployed in fishing ships sailing within the coast line of the Porto Metropolitan area, up to 10 nautical miles from shore [17].

In [18] the author performed Wi-Fi maritime communications tests using the TV White Spaces band (768 MHz). These tests were carried out using MARBED, which was also used in [19], where the author performed tests using the 5.8 GHz frequency band. The experimental results from [18] and [19] will be used to validate our simulation tool.

2.8 Network Simulators

In this section, some of the most popular network simulators tools are presented, including the one in which this MSc dissertation is based - ns-3.

2.8.1 ns-3 Simulator

The ns-3 simulator [20], is an open-source, discrete-event network simulator, targeted for research and educational purposes. It consists of a C++ library which provides a set of network simulation models implemented as C++ objects and wrapped through python, thanks to the *pybindgen* library. Users interact with this library by writing a C++ or a python application which instantiates a set of simulation models to set up the simulation scenario of interest, enters the simulation mainloop, and then exits when the simulation is completed.

The ns-3 offers models for devices and protocols for wired and wireless networks, IP and non-IP based. The main goal of the ns-3 project is to have a solid simulation core that is simple to use

and debug, thanks to the great documentation available, in order to satisfy the needs of a simulation workflow. This software encourages its large community to improve its models, by letting them to validate and maintain the existing models, thus allowing the development of new models that will fill the existing needs of simulating new communication protocols and environments. And that leads us to the main point of this MSc dissertation, which is the development of a unique model that simulates maritime networks, using ns-3.

2.8.2 QualNet Simulator

The Qualnet simulator is a commercial planning, testing and training tool that "mimics" the behavior of a real communications network [21], which contains a set of libraries for wireless and mobile network simulations. This simulator supports real-time speed, scalable simulation, with highly detailed models, plus having the capability of running in numerous platforms and connecting to other hardware and software applications. This simulator allows its users to develop and optimize new protocol models and to improve the existing ones, by providing the design of large wired and wireless networks using the models that they are developing or improving.

In the TRITON project [10], to fully understand and help in the design of the networking protocols, a framework for simulating wireless communications in the sea environment was developed [7], implemented over the QualNet simulator. This framework incorporated three unique maritime features: the wave motion and its effect on wireless transmissions, the sea surface path loss characteristics, and the mobility pattern of the ships.

For the wave motion and its effect on wireless transmissions, a traveling wave formula to approximate the shape of the waves and to estimate the degree of tilt in ships was used. Equation 2.13 gives the ship's effective height, where t is the time, x the distance from a common origin, λ the average sea wavelength, T the average wave period, and a and b are constants that control the height of the simulated waves. In [7] the authors have used $a = \frac{\lambda}{2\pi}$ and $b = H/2$, with H being the significant wave height, which is the average height (trough to crest) of the one-third highest waves, in order to approximate the wave to a trochoid, whose properties are known to mirror the sea waves.

$$y = a - b \times cos(x/\lambda - t/T) \tag{2.13}$$

The ship's tilt is given by Equation 2.14 where $x_{bow} = x + 1/2$, and $x_{stern} = x - 1/2$, are the ship's bow and stern position projected in the direction of the wave, and y_{bow} and y_{stern} are obtained trough equation 2.13 using x_{bow} and x_{stern}.

$$\theta = arctan(\frac{y_{bow} - y_{stern}}{x_{bow} - x_{stern}}) \tag{2.14}$$

The ship length, L, and the ship width, W, and the angle between the direction of the ship and the direction of the wave, α, allows to obtain $l = Lsin(\alpha)$ if $Lsin(\alpha) > W$, otherwise $l = Wcos(\pi/2 - \alpha)$.

Equation 2.15 represents the two-ray propagation loss model used, where d is the distance between the antennas, λ is the transmission wave length, h_t is the height of the transmitting antenna and h_r is the height of the receiving antenna. P_r and P_t are receiving and transmitting powers, and their ratio represents the power loss.

$$\frac{P_r}{P_t} = (\frac{\lambda}{4\pi d})^2 \times sin^2(\frac{2\pi h_t h_r}{\lambda d}) \tag{2.15}$$

To simulate the ships movement, statistical information from the ship traces was gathered, thus allowing to reach the best-fitted curve $p(x) = a \times b^x$, where $a \simeq 0.292$ and $b \simeq 0.998$.

To verify the correctness of this simulation model, the outcome of the simulation under similar sea conditions was compared with the available experimental observations. Figure 2.11 shows the experimental results, a), and the simulation results, b).

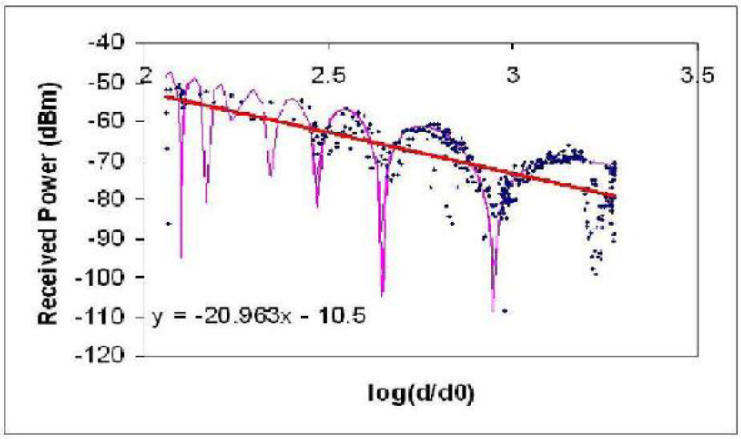

(a) Experimental result fitted with the theoritical curve

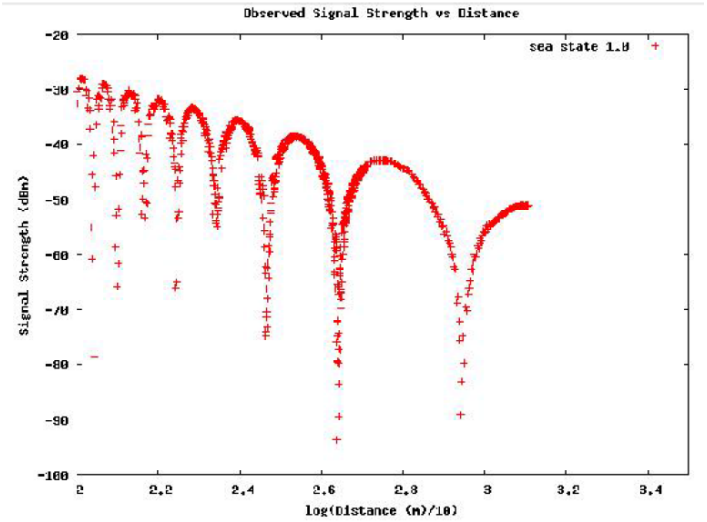

(b) Simulation result using the ocean terrain model

Figure 2.11: Comparison between experimental and simulation results [7]

Both graphics are very similar, being the only difference between them the value of signal strength at the receiver. This results from the fact that the transmission power and antenna in the simulation did not match those used in the experiment. Nonetheless, these differences in the received power did not affect the correctness of the path loss characteristics simulated, as the result showed that the simulation produced the drops in signal, as seen in the experiment.

2.8.3 Riverbed Modeler

The Riverbed Modeler is based on the OPNET Simulator, that was bought by Riverbed in 2012. It is a commercial discrete event-simulation engine for analyzing and designing communication networks [22]. This simulator allows the analysis of wired and wireless networks, considering different scenarios, including scalability simulation, using very reliable models. Using this simulator, the users can develop and evaluate new proprietary protocols or enhancements to the existing ones, being capable to test and demonstrate their ideas.

Although there is no known model for this simulator, regarding maritime communications, as we saw in Section 2.2, the propagation models available in the OPNET Simulator where used to compare with the developed two-ray model proposed in [2], thus allowing its authors to conclude that their propagation model was better suited for the maritime communication environment.

2.9 Summary

In this chapter, the research work that has been done in maritime wireless communications was presented. It was possible to understand the factors that affect the maritime wireless communications, thus proving these effects with some experimental results. The two-ray pathloss model presented in Section 2.2 allowed to better describe the behaviors of the radio signals in this environment. In Section 2.3 the ways of modeling the sea waves movement were presented, thus helping to accurately simulate the movements of the sea waves.

Some land-sea wireless communications projects were presented, thus helping to understand the best ways to have wireless communications in the maritime environment, and at the same time the challenges that emerged and ways to solve them.

Finally, we saw some of the most popular network simulators, including ns-3 in which this work is based on. Also, we referred an implementation of a model for maritime communications, based on the QualNet simulator. This last section helped us to conclude that the few network simulators that have models for the maritime communications are proprietary. There is no open source model for this kind of networks at the moment.

Chapter 3

Developed Simulation Tool for Maritime Wireless Networks

In this chapter we describe the new ns-3 based simulation tool developed for TCP/IP Maritime Wireless Networks. Firstly, we present the ns-3 architecture, focusing on the layers that were modified, in order to develop our simulation tool. Then, we detail the new propagation and mobility models implemented over ns-3, describing the decisions made during their development, along with their main features.

3.1 Ns-3 Architecture

Ns-3 is divided in multiple modules, as show in Figure 3.1. The ns-3 propagation and mobility modules (shown in green in Figure 3.1) were modified to implement the new ns-3 based simulation tool. The propagation module is responsible for modeling the propagation loss and delay. As for the mobility module, it tracks and maintains the current position and speed of a node, and includes helper classes to place nodes and setup mobility models.

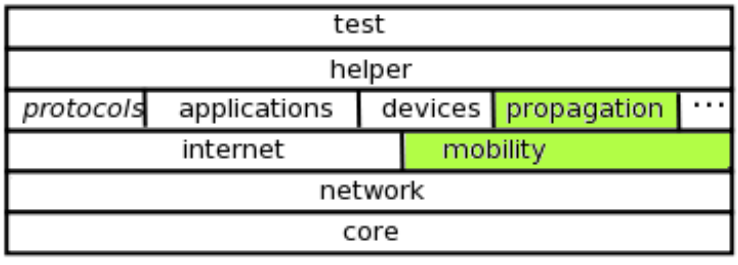

Figure 3.1: ns-3 Architecture (adapted from [8])

The class ns3::TwoRayMaritimeModel was created in the ns-3 propagation module, in order to implement the maritime propagation loss model and the class ns3::MaritimeOscillationModel

was created in the ns-3 mobility layer, for the implementation of the maritime mobility model. Both are detailed in Section 3.2 and Section 3.3.

3.2 Two-ray Maritime Model

The simulation tool needs to be able to predict the signal attenuation. For that purpose, the ns3::TwoRayMaritimeModel class was created, according to the UML architecture in Figure 3.2.

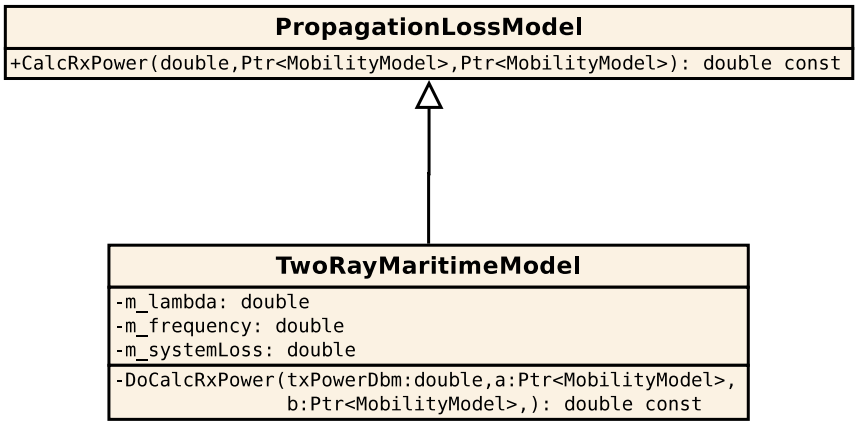

Figure 3.2: UML architecture of the Two-ray Maritime Model

The developed class has DoCalcRxPower() as its major function, and *m_lambda*, *m_frequency* and *m_systemLoss* as its major attributes. It inherits from the ns3::PropagatioLossModel class.

The DoCalcRxPower() function is responsible for calculating the receiver power, by estimating the pathloss, which is accomplished through the Two-ray Maritime Model in Equation 2.7. Equation 2.7 only requires information about the nodes position and the carrier frequency, which allows obtaining the carrier wavelength as this is equal to the speed of light in vacuum divided by the carrier frequency. Therefore, the frequency was defined as a private attribute of the model, *m_frequency*, along with the wavelength parameter, *m_lambda*, which is calculated right after the frequency is set. As for the nodes position, the DoCalRxPower() function receives as input the pointers of the mobility model of both nodes, which allows to extract the information about the nodes cartesian coordinates, thus also allowing to determinate the distance between them. Asides the signal attenuation, to calculate the received power, it is also needed the transmission power, which is given as an input of the DoCalRxPower() function. From the transmission power, we subtract the path loss, calculated through the two-ray pathloss equation, thus obtaining the received power. However, there are still some factors that can be taken into account. In any communications system there are always some losses due to the equipment and cables used. Therefore, to include those losses in our model, we created a private attribute, *m_systemLoss*.

In the maritime communications environment, there are three different scenarios that affect the path loss [11]. The first scenario, consists in an open sea, where the two-ray pathloss model is suitable to determine the loss occurred. However, when near the shore, where we have hills and

cliffs, we must consider the reflections from rocks. In a sea port or harbor, where the environment is more populated, there is a large amount of reflecting rays from the surroundings. For these two scenarios, we needed to consider the component of the multipath fading. In order to include the multipath component, we added to the model a Rayleigh random variable. According to [11], this variable is best fitted for the sea port scenario, where there are more reflections. However, this can also be applied to the less populated scenarios, as we aimed to introduce some statistical variation in the model. That also allowed to model some propagation effects that we could not do otherwise, such as the effects caused by the antenna's tilt and the temporary reflections caused by some nearby ships and rocks. Equation 3.1 presents the probability density function of the Rayleigh distribution:

$$f(x;\sigma_r) = \frac{x}{\sigma_r^2} e^{-x^2/(2\sigma_r^2)}, x \geq 0 \tag{3.1}$$

where σ_r is the scale parameter of the distribution. Since ns-3 does not support the Rayleigh distribution, we considered an approximation by using the Weibull distribution, which is available in ns-3, modifying the shape, $k = 2$, and scale parameters, $\lambda = \sigma_r * \sqrt{2}$ [23].

Considering these two additional parameters, the value of the received power, Rx, given by our model is presented in Equation 3.2:

$$Rx = Tx - Loss2ray - SystemLoss + Rayleigh \tag{3.2}$$

where Tx is the transmission power, $Loss2ray$ is the value of the calculated pathloss, using the two-ray model, $SystemLoss$ is the sum of all losses in the system (equipment and cables) and $Rayleigh$ is the component of the Rayleigh fading.

3.3 Maritime Oscillation Model

If we observe an anchored ship on the sea, we will see that its movement, due to the waves oscillation, consists of up and down movements along the wave. Therefore, in order to model this type of movement, we needed to make the height of the node vary around its stationary position. In order to achieve that the ns3::MaritimeOscillationModel class was created, UML architecture in Figure 3.3. The ns3::MobilityModel class is the parent class of our developed class, which has Update() as its major function, with DoSetPosition(), DoGetPosition() and Sea_State() as helper functions. As for attributes, the major ones are m_helper, m_period, $m\_amplitude$, $m\_wavelength$, m_mode and m_sea_state.

The Update() function is responsible for calculating the position of the node at each instant. In order to calculate the node position, it uses the oscillation models presented in Section 2.3, adding them to the default height of the node.

As there were two different mobility models available, we focused on the sine wave mobility model first, and then on the trochoid model, which is a more precise for high sea state levels, as discussed in Section 2.3. For the sine wave model, we used equation 2.8, which is known as

the traveling sine wave. To implement the trochoid oscillation model, we used the equation 2.11. In order to allow the user choose between the two models, we created a EnumValue parameter, named *Model_Mode*, which had two values, one for using the sine wave model, *MODE_SINE*, and the other for the trochoid wave model, *MODE_TROCHOID*.

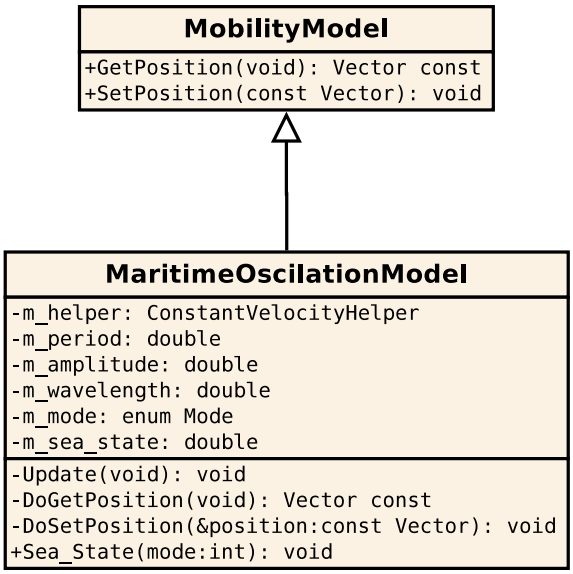

Figure 3.3: UML architecture of the Maritime Oscillation Model

Both mobility models require information about the sea state, such as its wave amplitude, period and length. Therefore, the private attributes *m_amplitude*, *m_period* and *m_wavelength* were created for these three parameters, respectively. To handle the node's position, the model uses the private attribute *m_helper*, from mobility helper class ns3::ConstantVelocityHelper, that stores information about the cartesian coordinates and velocity of the node. This helper class attribute is updated each time the node's new height is calculated, using the selected mobility model.

To ensure that the position of the node is constantly updated, at the end of this function, we schedule the simulator to call again this function, 0.1 seconds later, as shows the code snippet in Listing 3.1. In this way, the simulation works as it was in a loop, always calling this function to update the height of the node.

Listing 3.1: Simulator Schedule()

```
Simulator::Schedule(Seconds(0.1),
&MaritimeOscilationModel::Update, this);
```

When defining a simulation setup, using the ns3::MobilityHelper class, we can only choose one mobility model to use on all nodes. Therefore, to allow having a node stationary on shore and at the same time one moving in the sea, along the wave motion, we modified the mobility oscillation model so that it can simulate both cases. To do so, we defined the shore as the starting point of the X axis, and so, a node with X coordinate positive means that it is on the sea, and

therefore, moving according to the oscillation model. Otherwise, if the node's X coordinate is zero or negative, the model considers that the node is stationary, and so its position will not be updated.

The Pierson-Moskowitz sea state table, presented in Section 2.3, classifies the sea conditions in 10 levels, giving us the interval values of the wave period, amplitude and length, for each level. In order to allow the user to use a preset sea condition, we added the Sea_State() function that permits the characterization of the sea state, according to Table 2.1 upon receiving the *mode* number. This is done by redefining the attribute *m_sea_state*. Upon the initialization of the model, it calls the Sea_State(), giving it the value of *m_sea_state*, which should vary from -1 to 9, where -1 means that the values are defined by the user, and 0 through 9 equals a sea level on Table 2.1. According with the value of *m_sea_state*, the function uses a switch case to determine and set the values of *m_amplitude*, *m_period* and *m_wavelength*, through the ns3::UniformRandomVariable class, which is an uniform distribution random number generator, that selects a value from the interval, corresponding to the defined sea state level.

3.4 Summary

In this chapter, we described the development of the simulation tool for maritime wireless networks. We started by describing the ns-3 architecture, focusing on the propagation and mobility models, which were improved with our developed models.

Then, we described the developed models, detailing their major functions and attributes. First, the Two-ray Maritime Model implemented on the propagation module in order to predict the signal attenuation in a maritime communication scenario, using the two-ray pathloss model in Equation 2.7. Then, the Maritime Oscillation Model implemented on the mobility module in order to model the movement of a node in the sea, using both mobility models presented in Section 2.3.

Chapter 4

Validation of the Simulation Tool for Maritime Wireless Networks

This chapter is devoted to the validation of the developed simulation tool. First, we describe the validation methodology, including the simulation scenarios and setups, carried out to validate the simulation tool. Then, we compare simulation results with experimental results obtained for the same communications scenarios. Finally, we wrap up this chapter by discussing the overall results.

4.1 Validation Methodology

After implementing the Two-ray Maritime Model and the Maritime Oscillation Model, presented in the Chapter 3, we needed to validate the models by comparing the simulation results with the experimental results published in the literature. In order to validate the developed models, the scenarios presented in Subsection 4.1.1 were considered, from which we developed the simulation setups described in Subsection 4.1.2, so that we could obtain simulation results to perform the comparison with experimental results in each scenario.

4.1.1 Simulation scenarios

The simulations were carried out considering the experiments for the 5.8 GHz frequency band [19] and 768 MHz (TV White Spaces) [18]. Both experiments consisted in the evaluation of the performance of a point-to-point link that was established between a fishing ship and shore, with each experiment having its own set of parameters. For [19], a transmission power of 20 dBm was used, where the transmitter and receiver antennas had gains of 16 dBi and 10 dBi and heights of 20 and 8 m, respectively. As for the experiment in [18], a transmission power of 28 dBm was used, where the transmitter and receiver antennas had gains of 9.8 dBi and 3.4 dBi and heights of 18 and 8 m, respectively. In both experiments the sea was relatively calm, between level 2 and 3 in the the Pierson-Moskowitz sea state classification.

Regarding the propagation model we have two scenarios where we can evaluate it, one for each of the frequency band used in the experiments. Besides the difference in the frequency used,

each experiment had different antennas, with different gains and transmission power. Therefore, we used these two scenarios to evaluate the developed propagation model. In both cases, the experiments consisted in having communications between two nodes, one stationary node on shore and the other moving away from shore on the sea. Therefore, the mobility model was responsible for replicating the experiment, making one of the nodes oscillate due to the sea waves. This caused the variation of the height of the sea antenna, thus adding more variability on the Two-ray Maritime Model.

As for the mobility model, both experiments had similar sea conditions. So, there was just one main scenario to evaluate the mobility model, which consisted in having one stationary node on the shore and the other moving away from shore, and oscillating in Z coordinate. However, there was still the possibility to compare the sine and trochoid models. But since, in the experiments performed in [18] [19], the sea was relatively calm, with low wave amplitude, there was no big difference using the sine wave or the trochoid model, as we explained in Section 2.3. The differences between these two models are only perceptible as the amplitude grows higher.

4.1.2 Simulation setups

In order to validate our simulation tool, we considered the simulation scenarios in Subsection 4.1.1 in order to develop different simulations setups, for measuring the following metrics: throughput, delay, jitter and RSSI. For each setup, we used the developed Two-ray Maritime Model, with the Rayleigh fading component set as default ($\sigma = 1$), as the propagation loss model and created two nodes, one static representing the shore node, and another representing the sea node, oscillating in the Z axis according to the sine wave model implemented on the developed Maritime Oscillation Model while moving away from the shore, as shown in Figure 4.1.

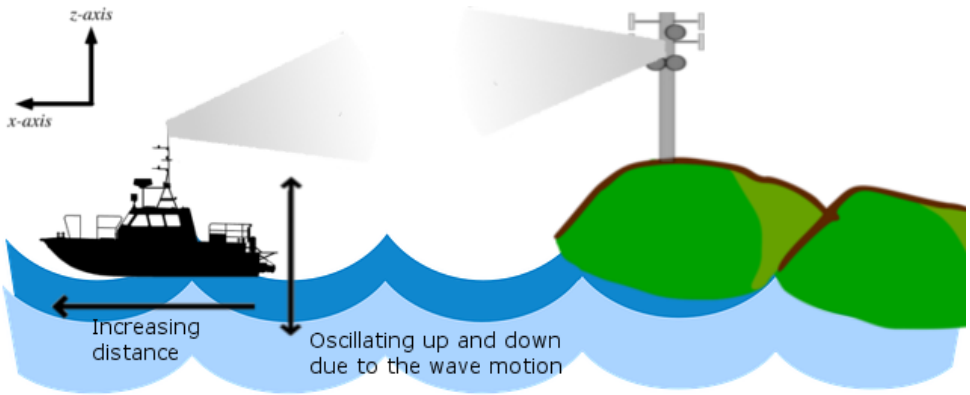

Figure 4.1: Representation of the simulations

The simulations were carried out for 5.8 GHz and 768 MHz, according to the experiments performed in [18] and [19] for the same communications scenario. The parameters considered in the experiments reported in [18] [19], such as the transmission power, transmitter and receiver

antenna's gains and heights and sea wave characteristics (period, amplitude and length), are presented in Table 4.1. Note that the values marked with an asterisk, were not available in the literature, and therefore we considered some suitable approximations. For the wave period for the 768 MHz scenario, we used the same value available in the 5.8 GHz scenario, given that in both cases the wave amplitude was almost the same. Regarding the wave length of both experiments, we approximated their value using the Pierson-Moskowitz sea state table. In the 768 MHz scenario, the path made by the boat was outside of the radiation area of the antenna, therefore the actual value considered for its was 0 dBi. The total system loss in both scenarios, was around 5 dB.

Parameter	5.8 GHz	768 MHz
Transmission power	20 dBm	28 dBm
Gain of transmitter	16 dBi	9.8 dBi
Gain of receiver	10 dBi	3.4 dBi
Height if transmitter	20 m	18 m
Height of receiver	8 m	8 m
Wave period	5 s	5* s
Wave amplitude	0.7 m	0.8 m
Wave length	10* m	10* m
Bit rate	6,5 Mbit/s	auto
Channel width	20 MHz	5 MHz
Modulation	802.11n	802.11bg

Table 4.1: Experimental Parameters

For measuring the throughput, delay and jitter, we considered a simulation setup with two nodes, where the shore node has the ns-3 OnOff application, while the sea node has the DataSink application, thus allowing to generate traffic between them. On top of that, we used Flow Monitor [24], an ns-3 tool that analyses all the network flow and enables the measurement of packet loss, throughput, delay and jitter during the simulation. In this setup, we repeated each simulation setup 10 times, with 10 different seeds, incrementing the sea node distance from the shore, at the end of each 10 seeds. It was used the 802.11 infrastructure mode and UDP as the transport protocol. In order to allow simulations of long range Wi-Fi links, we had to modify the ns3::WifiMac class. The ACK timeout and Slottime parameters were reconfigured in order to enable a link of up to 20 km.

In the delay and jitter simulations, the simulation time was set to 60 seconds, with the transmitter sending data during 30 seconds, with a bit rate of 1 Mbit/s, for the 5.8 GHz scenario, and 0.1 Mbit/s, for 768 MHz, in order to avoid an early channel saturation. Regarding the throughout, it was necessary to saturate the channel, since the measurement of throughput requires the nodes communicating at a higher bit rate. In the 5.8 GHz scenario, it was used a constant bit rate of 6,5 Mbit/s. For that purpose, we used the ns3::ConstantRateWifiManager class to have a constant 6 Mbit/s bit rate. As for the 768 MHz experiment, it used an automatic rate, and so we set the bit

* Approximated values, as they were not available in literature

rate to automatic using ns3::AarfWifiManager, saturating the channel at 6 Mbit/s. Given this increase in the bit rate on the throughput simulation, the simulation time was set to 30 seconds, with the transmitter sending data during 10 seconds, reducing the total simulation time for 10 seeds, without compromising the statistical relevance of the obtained results.

In order to measure the RSSI, we considered a different simulation setup since the Flow Monitor does not have the capability of measuring the RSSI. This setup consisted in calculating the mean value of the received power of 30 measurements done with the ns3::TwoRayMaritimeModel class, every second. During these 30 measurements, the sea node was stationary, but oscillating on the z-axis, due to the sea wave motion. After 30 measures, the sea node had its distance from shore incremented, and a new set of 30 measurements was made, and so on.

To evaluate the accuracy of the models and to see how close the simulation results were to the experimental, we estimated the error between results. That estimation was made by using the absolute difference between the curves of both simulation and experimental results, and then estimating the average of those errors.

4.2 Results with 5.8 GHz

In this section we present the simulation results for a long range Wi-Fi link in maritime environment operating at 5.8 GHz and compare them with the experimental results obtained in [19]. The simulations were carried out considering the parameters specified in Table 4.1. In the following subsection we present the simulation results in comparison with the experimental results, concerning the following metrics: RSSI, throughput, delay and jitter.

4.2.1 RSSI

Figure 4.2 presents the simulation results for the RSSI setup, in comparison with the experimental and theoretical RSSI.

The simulation results tend to be closer to the theoretical, which is due to the fact that the presented simulation RSSI results from the mean of thirty measures, therefore the mean value will tend to be closer to the theoretical value, since the simulation model uses the same two-ray equation as used for the theoretical values. The mean absolute difference of 2.7 dB in Table 4.2 can be explained by two factors. First, the fact that the theoretical results consider the same height of the sea node, 8 meters, while in the simulation this value varies between 7.3 and 8.7 meters, due to the sea wave oscillation. Another factor is due to the Rayleigh error component, which causes more statistical variation on the simulated RSSI.

Regarding the experimental results, as shown in Table 4.2, there is a 7 dB mean absolute difference which, not only can be justified by the two factors pointed out regarding the theoretical results, but also because there the experimental measurements were made, while the ship was moving, rather than with it stationed.

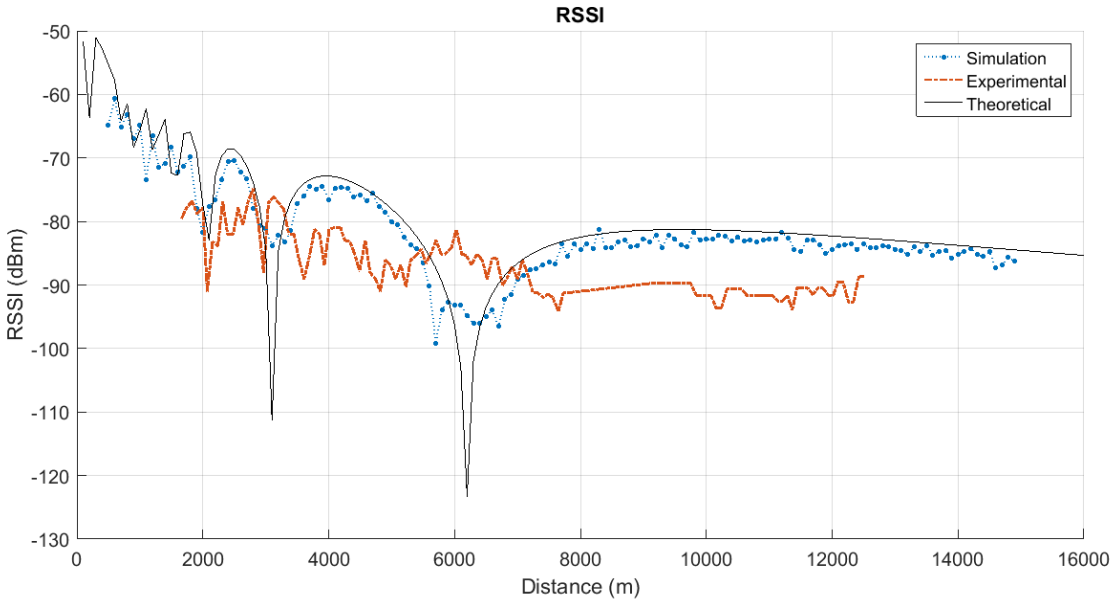

Figure 4.2: RSSI results for 5.8 GHz

Result	Difference
Experimental	7.0
Theoretical	2.7

Table 4.2: Mean absolute difference of the simulation RSSI, in dB

4.2.2 Throughput

Figure 4.3 shows the results from simulation throughput in comparison with the experimental throughput, including maximum and minimum values for both curves.

It is clear that both curves have little resemblance, considering the mean throughput values for each distance. However, observing the maximum and minimum values, we see that the experimental results had a big fluctuation, resulting in a smaller mean value when compared with the simulation results, which had the maximum and minimum with little variation, which translated in a bigger mean value of the throughput, around 4 Mbit/s until 5 km. Both curves have a similar tendency until 6 km, where they hit their respective minimum. But from here on the experimental throughput kept around zero, while the simulation throughput increases. This can be explained by looking at the RSSI plot of Figure 4.2. We see that near 6 km the simulation RSSI drops below -90 dBm, making it impossible to have a proper communication link. As such, we got low throughput values, as expected. Right after this zone, the RSSI values rise again, which also made the throughput rise. However, looking at the experimental RSSI we see that it kept around -90 dBm, explaining why there was no longer experimental throughput after the 6km.

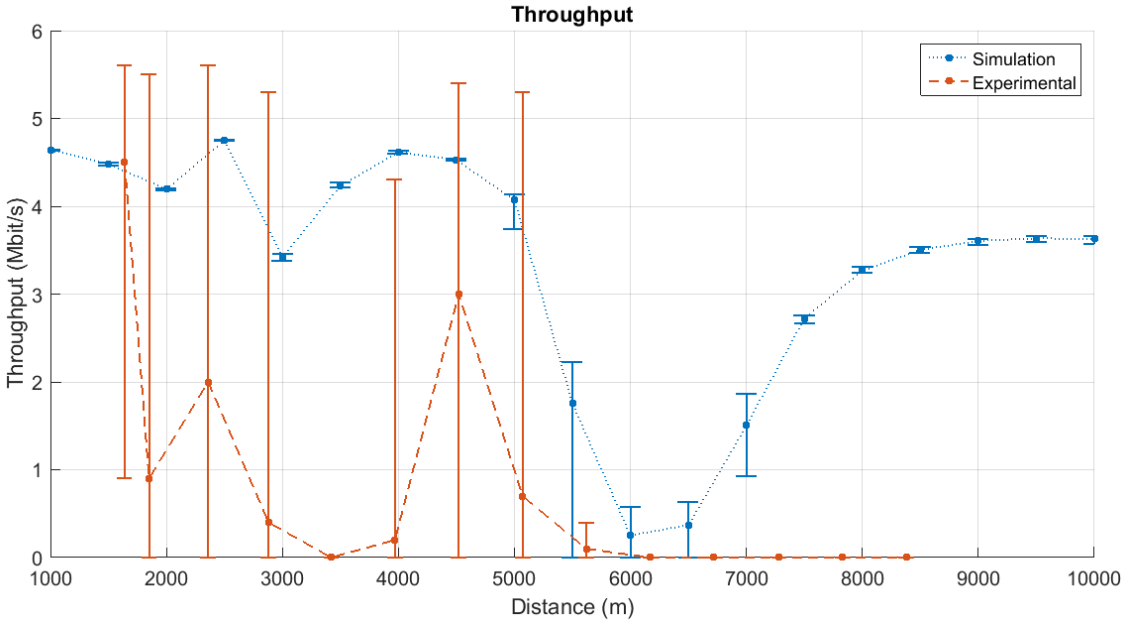

Figure 4.3: Throughput results for 5.8 GHz

4.2.3 Delay

Figure 4.4 shows the delay results obtained in simulation in comparison with the experimental delay, including maximum and minimum values for both curves.

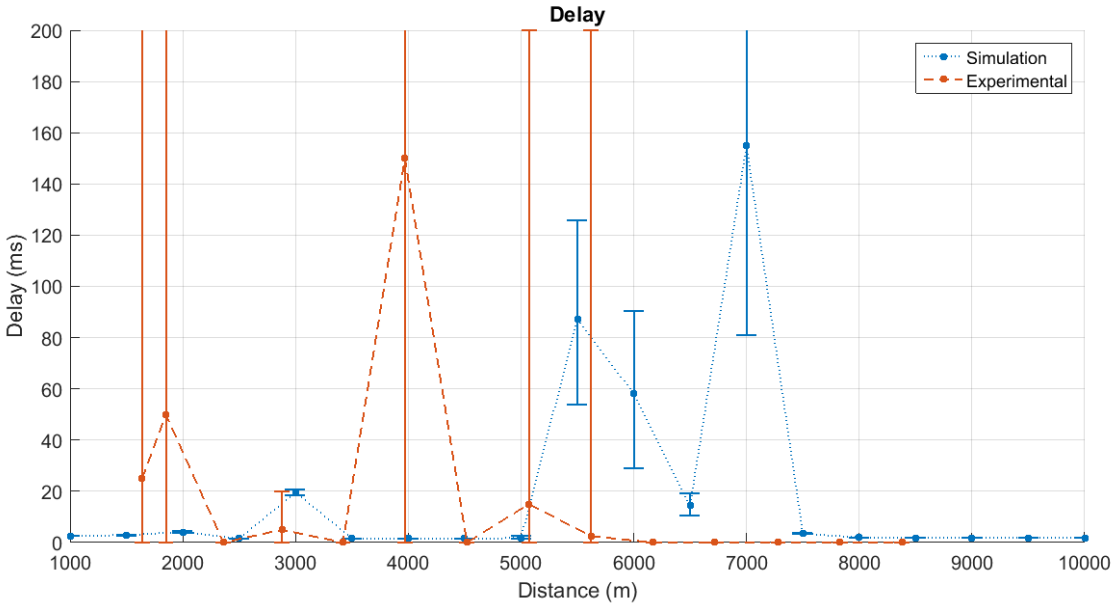

Figure 4.4: Delay results for 5.8 GHz

By analysing both curves we see that both are similar, having some peaks where the delay is high, with big fluctuation between minimum and maximum values. However, the simulation curve has some temporal offset from the experimental curve, regarding the peaks. These sudden delay peaks match the behaviour observed regarding the throughput in Figure 4.3, given the fact that in those points the RSSI has a peak. And again we observe the distinct behaviour in both curves after the 6 km distance, the simulation still some peaks, while the experimental delay ceases to exist, as result of the RSSI being around -90 dBm, which made impossible to establish communication.

4.2.4 Jitter

Figure 4.5 shows the jitter results for simulation in comparison with the jitter obtained experimentally in [19], including maximum and minimum values for both curves.

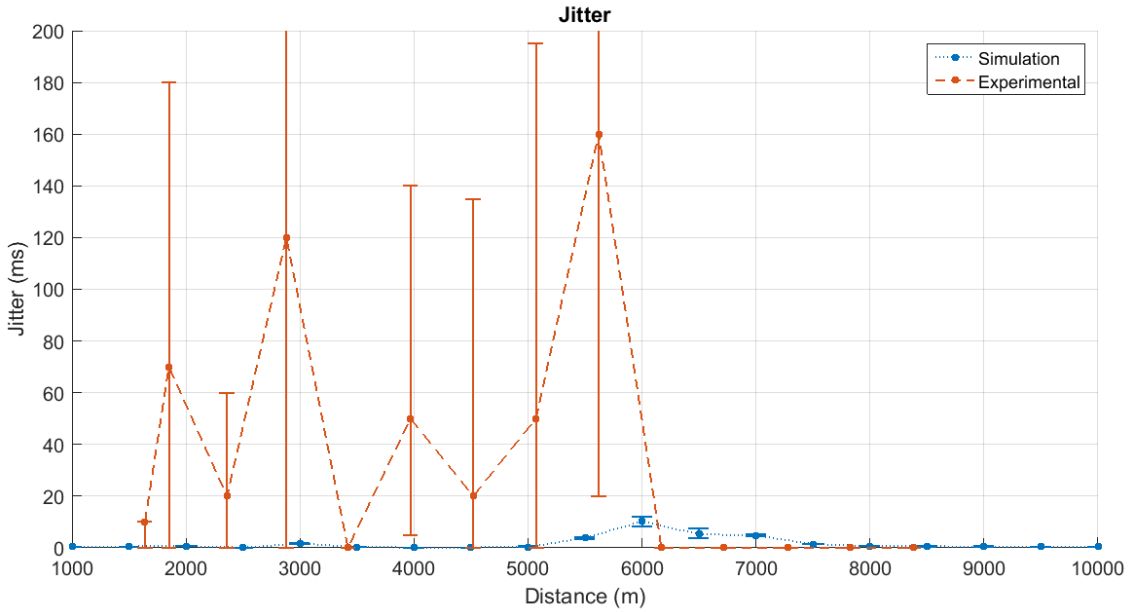

Figure 4.5: Jitter results for 5.8 GHz

In this case, we observe a big fluctuation on the experimental results, while the simulation results have little variation. Since the jitter depends on the variation of the delay, in each set of measurements, the simulation results proved that the difference on the simulation delay was not of the same magnitude as the difference occurred experimentally. It is still possible to note some small peaks on the simulation jitter, which coincide with the distances where we got the bigger delay peaks. However, these jitter peaks are not close to those registered experimentally. This small simulation delay variation and therefore small jitter, in comparison with the experimental, can be explained by the fact that the simulation measurements were carried with the node stationed at each position, while in the experiment the ship was moving, while the measurements were being

done, which causes much more communication inconsistencies, and therefore affecting the delay and jitter.

4.3 Results with 768 MHz

In this section we present the simulation results for a long range Wi-Fi link in maritime environment operating at 768 MHz and compare them with the experimental results obtained in [18]. The simulations were carried out considering the parameters specified in Table 4.1. In the following subsection are presented the simulation results in comparison with the experimental results, concerning the following metrics: RSSI, throughput, delay and jitter.

4.3.1 RSSI

Figure 4.6 presents the RSSI simulation results in comparison with the experimental RSSI measured in [18], along with the theoretical RSSI curve.

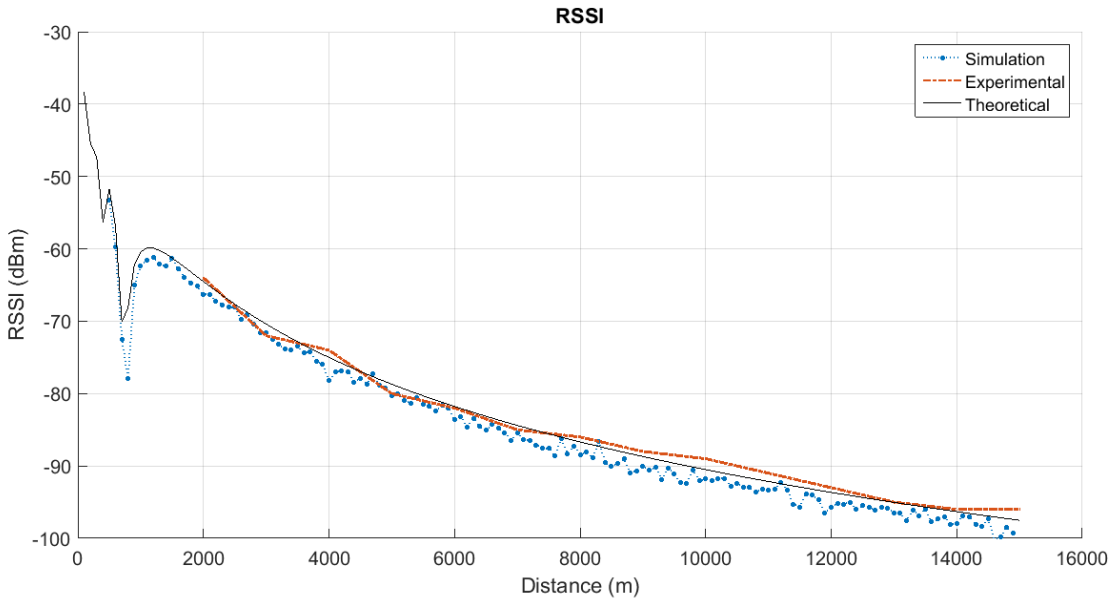

Figure 4.6: RSSI results for 768 MHz

As we can see, the three curves are very close to each other, proving that the simulation tool successfully models the RSSI in this scenario. The mean absolute differences in Table 4.3, indicates a 2 dB difference between the simulation and experimental results, which can mostly be justified by the variations caused by the height of the ship antenna and also due to the Rayleigh random factor. Regarding the theoretical results, the simulation RSSI is even closer, which is expected as they are both calculated using the same equation, differing on the fact that the simulation has the Rayleigh component, and also the height variation.

Result	Difference
Experimental	2.0
Theoretical	1.5

Table 4.3: Mean absolute difference of the simulation RSSI, in dB

4.3.2 Throughput

Figure 4.7 shows the throughput results obtained by using simulation as well as the experimental throughput, reported in [18], including maximum and minimum values for the both curves. The simulation curve starts at 6 Mbit/s rapidly decreasing, approximating to the experimental curve. Given the RSSI curves in Figure 4.6, it was expected that both throughput curves were similar, which only happens around the 6 km. Since it was used an automatic rate, in the experiment the throughput was lowered to face the adversities existing on the communication link, that were not modeled in simulation, and therefore there was more bit rate available.

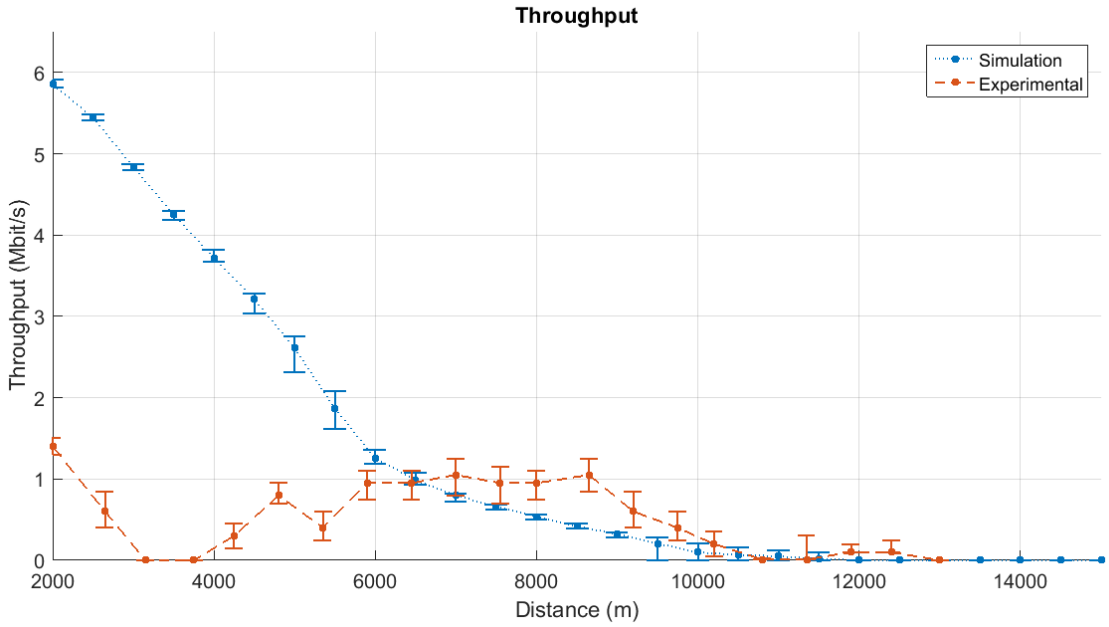

Figure 4.7: Throughput results for 768 MHz

4.3.3 Delay

Figure 4.8 shows the delay results from simulation in comparison with the experimental delay, including maximum and minimum values only for the simulation curve, since the experimental maximum and minimum values were not available in literature.

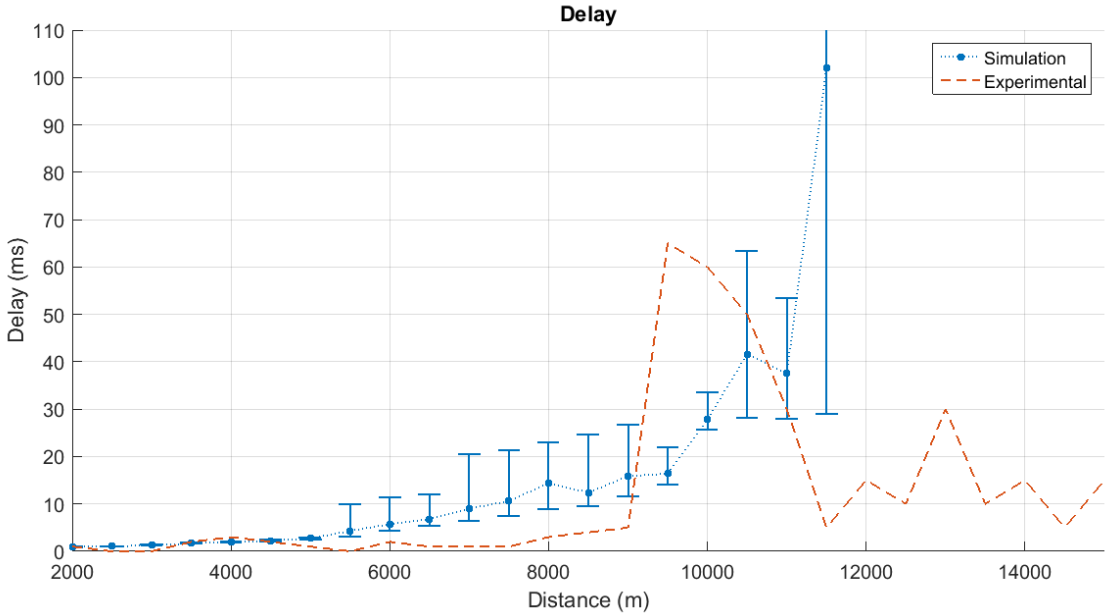

Figure 4.8: Delay results for 768 MHz

Until 5 km, both curves have similar values close to zero milliseconds. After that distance both curves began to show different behaviours. The simulation curve, starts to show more fluctuation on the maximum and minimum values, with a overall mean value increase in comparison with the experimental curve. After 9 km, the simulation curve presents a bigger increase, while the experimental curve starts to present some delay peaks. After 11 km, the simulation delay ceases to exist due to the channel saturation, while the experimental peaks stabilize.

4.3.4 Jitter

Figure 4.9 shows the jitter results obtained in simulation and experimentally, including maximum and minimum values only for the simulation curve, since the experimental maximum and minimum values were not available in literature.

In these results, we have a big difference between simulation and experimental results. The simulation curve steadily increases until 12 km where the channel becomes saturated, and therefore there was not possible to measure the delay and jitter from there on. On the other hand, the experimental curve shows various peaks, which can be explained by the ship moving while the experimental measurements were being done, causing communication inconsistencies, and therefore affecting the delay and jitter.

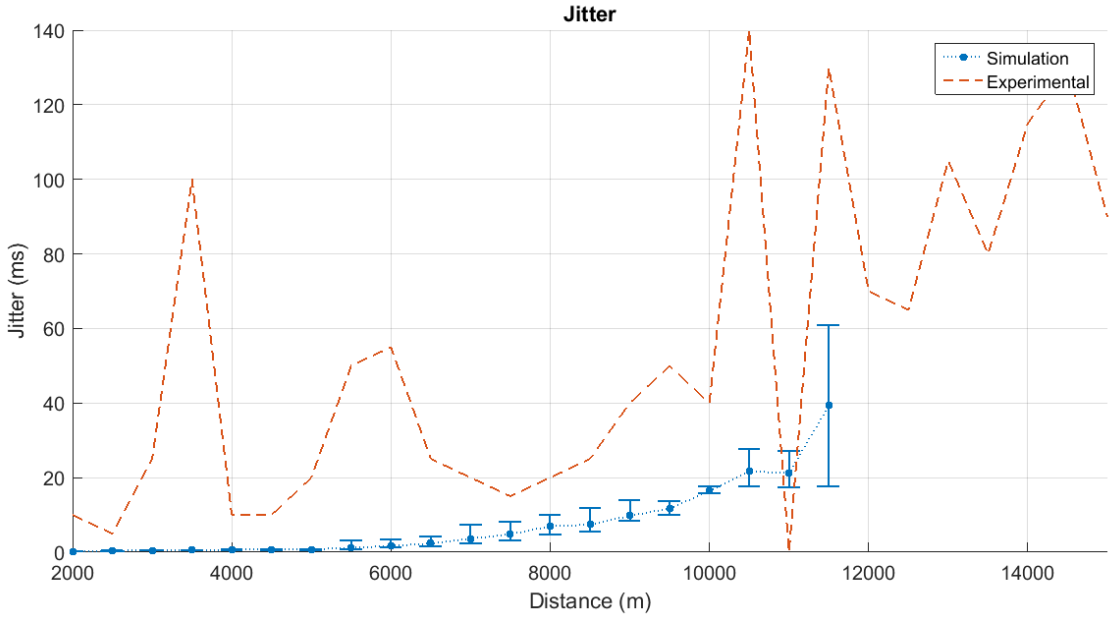

Figure 4.9: Jitter results for 768 MHz

4.4 Discussion

Regarding the RSSI results, we can conclude that the simulation tool was capable of modeling the RSSI in both 5.8 GHz and 768 MHz experiments. In both cases the simulation results were closer to the theoretical than the experimental results, which was expected given that they use the same equation as basis to calculate the RSSI, with the simulation having more variation due to the Rayleigh component. Regarding the experimental results, there were two different situations. In the 5.8 GHz experiment, the results had a 7 dB difference from the simulation results, which can be explained by the fact that the RSSI experimental measurements were carried while the ship was moving, which caused it to not present those characteristic deep holes as shown in the theoretical curve. On the other hand, the simulation curve tends to be close to the theoretical curve, but not showing deep holes due to the fact that the simulation results come from the mean of thirty measurements. The small difference between simulation and theoretical results is mainly due to the Rayleigh component, but also due to the height variation of the sea node, oscillating along the wave. As for the 768 MHz scenario, all the three curves are close, following the same tendency, with a 2 dB difference between simulation and experimental results.

In the throughput results, there was a similar tendency in both scenarios. The simulation curves started with values above the experimental, and then an approximation happened. In the 5.8 GHz scenario, that approximation was followed by the departure of both curves, as the simulation throughput increased, following the tendency of its RSSI curve. In the 768 MHz scenario, the simulation curve is similar to the experimental curve. From both experiments, we can conclude that the initial throughput, obtained in simulation, is too optimistic, as the simulation does not

recreate some adversities that are faced on the experiments. However, as the distance increases the simulation throughput tends to be more realistic.

The delay obtained in the simulation for 5.8 GHz, shows a similar behaviour as the experimental results, as both present some time to time peaks, with the particularity of having a little temporal offset. Given this scenarios, we can conclude that the simulation delay was close to representing the reality. In the 768 MHz scenario, we observed that until 9 km simulation results had a similar tendency to the experimental results, with low delay values, but with the simulation curve starting to present some fluctuations closer to that distance. From there on, the simulation curve has a bigger increase until 11 km, where the channel becomes saturated and therefore no more measurements were possible. On the other hand, after 9 km, the experimental curve presents some peaks. We can conclude that the simulation tool was able to model most of the delay observed experimentally, but with some differences regarding the delay peaks.

Concerning the jitter experiments, in both cases the obtained simulation results were not close to the experimental. The simulated delay was too small, which can be explained by the fact that the simulation measurements were carried with the node stationed at each position, while in the experiment the ship was moving during the measurements. This causes much more communications inconsistencies, and therefore induces more delay variations, meaning higher jitter. From this we can conclude that it is necessary to do simulations with the nodes moving, instead of them being stationary, in order to obtain more accurate results.

Chapter 5

Conclusion

This dissertation arises in the context of maritime wireless communications. The main goal was to develop a simulation tool for TCP/IP maritime wireless networks based on ns-3.

The state of the art solutions still have many challenges to establish low cost and high bandwidth maritime wireless communications. During the literature review we found some projects that are trying to overcome them. In addition, we presented theoretical models that enable the simulation of the signal propagation in the sea environment and the ocean surface movement. We finalized Chapter 2 by describing the ns-3 characteristics and other similar simulation tools, plus some proprietary models done for them, regarding the maritime communications, whose support is lacking in ns-3.

The new ns-3 models developed during this MSc dissertation enhance ns-3 with the capability of simulating TCP/IP maritime wireless networks. In order to achieve that, the Two-ray Maritime Model was created, in order to allow the prediction of the signal attenuation in a maritime communications scenario. Along with this model, the Maritime Oscillation Model was also created in order to model the movement of a node in the ocean.

The validation of the developed models, comparing simulation results with experimental results considering the same conditions, proved the accuracy of the developed simulation tool for maritime wireless networks. Yet, there are still some features that can be included as future work, such as:

- Improve the mobility model, by using a sum of multiple sine/trochoid waves, allowing a better representation of the sea, as it is composed by multiple waves, rather than a single one;
- Add the boat/antenna tilt feature to the mobility model, by calculating the tangent of the ship of relatively to the ocean wave;
- Allow to have the node moving at a constant speed, thus allowing to perform measurements while the node is moving, away from shore, instead of only performing measurements with the node stationed in a given position;

- Classify the nodes by defining different ship sizes, meaning a different height of the antenna, and the variation pathloss component caused by signal reflection and blockage from the ship;
- Evaluate the performance of the trochoid and sine wave models in a more agitated ocean, with bigger wave amplitude, where the trochoid model should present a better accuracy than the sine model;
- Evaluate the performance of the maritime communications in a multi-hop network.

References

[1] Chee-Wei Ang and Su Wen. Signal strength sensitivity and its effects on routing in maritime wireless networks. In *Local Computer Networks, 2008. LCN 2008. 33rd IEEE Conference on*, pages 192–199. IEEE, 2008.

[2] Rosario Giuseppe Garroppo, Stefano Giordano, and Davide Iacono. Experimental and simulation study of a wimax system in the sea port scenario. In *Communications, 2009. ICC'09. IEEE International Conference on*, pages 1–5. IEEE, 2009.

[3] HyperPhysics. Ocean Waves, December 2014. http://hyperphysics.phy-astr.gsu.edu/hbase/waves/watwav2.html, last visited at 7 December 2014.

[4] Sébastien Thon and Djamchid Ghazanfarpour. Ocean waves synthesis and animation using real world information. *Computers & Graphics*, 26(1):99–108, 2002.

[5] J Joe, SK Hazra, SH Toh, WM Tan, J Shankar, Vinh Dien Hoang, and Masayuki Fujise. Path loss measurements in sea port for wimax. In *Wireless Communications and Networking Conference, 2007. WCNC 2007. IEEE*, pages 1871–1876. IEEE, 2007.

[6] YoungBum Kim, JongHun Kim, YuPeng Wang, KyungHi Chang, Jong Won Park, and YongKon Lim. Application scenarios of nautical ad-hoc network for maritime communications. In *OCEANS 2009, MTS/IEEE Biloxi-Marine Technology for Our Future: Global and Local Challenges*, pages 1–4. IEEE, 2009.

[7] Su Wen, Peng-Yong Kong, Jaya Shankar, Haiguang Wang, Yu Ge, and Chee-Wei Ang. A novel framework to simulate maritime wireless communication networks. In *OCEANS 2007*, pages 1–6. IEEE, 2007.

[8] Ns-3 manual, February 2015. http://www.nsnam.org/docs/manual/html/.

[9] Magalhães João. Mac for wi-fi-based land-sea communications. Master's thesis, Faculdade de Engenharia da Universidade do Porto, 6 2014.

[10] Jaya Shankar Pathmasuntharam, Peng-Yong Kong, Ming-Tuo Zhou, Yu Ge, Haiguang Wang, Chee-Wei Ang, Wen Su, and Hiroshi Harada. Triton: High speed maritime mesh networks. In *Personal, Indoor and Mobile Radio Communications, 2008. PIMRC 2008. IEEE 19th International Symposium on*, pages 1–5. IEEE, 2008.

[11] Ming-Tuo Zhou and Hiroshi Harada. Cognitive maritime wireless mesh/ad hoc networks. *Journal of Network and Computer Applications*, 35(2):518–526, 2012.

[12] PHYSCLIPS. Travelling Sine Wave, JUNE 2015. http://www.animations.physics.unsw.edu.au/jw/travelling_sine_wave.htm.

[13] Namkyung Lee, Nakhoon Baek, and Kwan Woo Ryu. A real-time method for ocean surface simulation using the tma model. *International Journal of Computer Information Systems and Industrial Management Applications (IJCISIM)*, 1:15–21, 2009.

[14] J Joe, SK Hazra, SH Toh, WM Tan, and J Shankar. 5.8 ghz fixed wimax performance in a sea port environment. In *Vehicular Technology Conference, 2007. VTC-2007 Fall. 2007 IEEE 66th*, pages 879–883. IEEE, 2007.

[15] Infocomm Development Authority of Singapore. First In The World: Wireless Mobile Wimax Access In Singapore's Seaport Now A Reality, December 2014. https://www.ida.gov.sg/About-Us/Newsroom/Media-Releases/2008/20080306142631.

[16] Christopher D Moffatt. High-data-rate, line-of-site network radio for mobile maritime communications (using harris wetnet technology). In *OCEANS, 2005. Proceedings of MTS/IEEE*, pages 1–8. IEEE, 2005.

[17] Tec4Sea. MARBED - MARitime wireless networks testBED, February 2015. http://www.tec4sea.com/the-research-infrastructure/resources/marbed-maritime-wireless-networks-testbed.

[18] Silva Santos Luciano. Wi-fi maritime communications using tv white spaces. Master's thesis, Faculdade de Engenharia da Universidade do Porto, 7 2013.

[19] Matos Lopes Mário. Comunicações marítimas wi-fi usando a banda 5.8 ghz. Master's thesis, Instituto Superior de Engenharia do Porto, 10 2013.

[20] ns-3, December 2014. http://www.nsnam.org/.

[21] SCALABLE Network Technologies. QualNet, December 2014. http://web.scalable-networks.com/content/qualnet.

[22] Riverbed. Riverbed Modeler, December 2014. http://www.riverbed.com/products/performance-management-control/network-performance-management/network-simulation.html.

[23] P Mohana Shankar. *Fading and shadowing in wireless systems*. Springer Science & Business Media, 2011.

[24] Gustavo Carneiro, Pedro Fortuna, and Manuel Ricardo. Flowmonitor: a network monitoring framework for the network simulator 3 (ns-3). In *Proceedings of the Fourth International ICST Conference on Performance Evaluation Methodologies and Tools*, page 1. ICST (Institute for Computer Sciences, Social-Informatics and Telecommunications Engineering), 2009.